# Hydrodynamic Modeling of Coronal Plasma and Comparison with Observations

F. Reale, G. Peres, R. Betta

*Istituto ed Osservatorio Astronomico di Palermo, Piazza del Parlamento 1, 90134 Palermo, Italy*

**Abstract.** We show that hydrodynamic modeling coupled to the synthesis of the plasma emission, taking into account the response of a given instrument, provides very useful information for the interpretation of flaring coronal loops observed in the X-ray band. We show how the same model flare would appear very different if observed with Yohkoh SXT and TRACE and how our approach can help in providing a very detailed plasma diagnostics for such observations.

## 1. Introduction

Hydrodynamic modeling is a well established approach to studying the physics of plasma magnetically confined in coronal loops. Plasma inside loops macroscopically behaves like a fluid and its structure, dynamics and evolution can be described in many respects using pure hydrodynamics, since mass, momentum and energy transport occurs mostly along the magnetic field lines: we neglect direct effects of magnetic field except for the geometric confinement.

Coronal loops are often the site of highly dynamic and transient phenomena, such as brightenings and flares, which need to be studied using time-dependent hydrodynamic models. These models imply the numerical solution of the fluid conservation equations and many of them have been developed and extensively used in the past (cf. Kopp et al. 1986). The models yield the evolution of plasma physical quantities, i.e. temperature, density and velocity, along the loop, which can be used to interpret the observations.

In order to perform a punctual, detailed and quantitative comparison of the model results to observational data, our approach to loop hydrodynamic modeling traditionally includes the synthesis from the physical quantities of the plasma emission taking into account the spectral and spatial response of the instrument used for the observation (e.g. Peres et al. 1987, Reale & Peres 1995). We consider this as an essential step of the study of the specific event, since the spectral response of the given instrument is generally highly non-linear with temperature and its coupling to the proper plasma emission evolution, associated with the plasma evolution and dynamics, makes the interpretation of an observation absolutely untrivial.

This will be shown in the following with the specific example of a flare model: it will be shown how the same (model) flare may appear very different when observed with two different coronal telescopes, the currently operative

Yohkoh SXT and the forthcoming TRACE, due to their very different spectral response.

In section 2 we describe our approach to modeling, in section 3 we show the results for the model flare, in section 4 we briefly discuss the results.

## 2. The modeling

The basic assumption of our modeling of coronal loops is that plasma is confined inside a semicircular rigid coronal loop with constant cross-section. Mass and energy transport occurs only along the magnetic field lines, so that we can adopt a purely hydrodynamic and one-dimensional description.

Let's now consider a compact flare in a closed loop. This highly dynamic event requires the solution of the time-dependent hydrodynamic equations for a compressible plasma, including effects such as solar gravity, plasma classical viscosity and heat conduction, and radiative cooling from an optically thin plasma (Raymond & Smith 1977):

$$\frac{dn}{dt} = -n\frac{\partial v}{\partial s} \tag{1}$$

$$n m_H \frac{dv}{dt} = -\frac{\partial p}{\partial s} + n m_H g + \frac{\partial}{\partial s}\left(\mu \frac{\partial v}{\partial s}\right) \tag{2}$$

$$\frac{d\mathcal{E}}{dt} + w\frac{\partial v}{\partial s} = \mathcal{Q} - n^2 \beta \mathcal{P}(T) + \mu\left(\frac{\partial v}{\partial s}\right)^2 + \frac{\partial}{\partial s}\left(\kappa \frac{\partial T}{\partial s}\right) \tag{3}$$

$$p = (1+\beta) n k_B T \qquad \mathcal{E} = \frac{3}{2}p + n\beta\chi \qquad w = \frac{5}{2}p + n\beta\chi \tag{4}$$

where $n$ is the hydrogen particle density, $t$ the time, $s$ the coordinate along the loop, $v$ the plasma velocity, $T$ the temperature, $p$ the pressure, $g$ the gravity, $m_H$ the hydrogen atomic mass, $\mu$ the viscosity, $\beta$ the ionization fraction, $\kappa$ the thermal conductivity, $\chi$ the hydrogen ionization potential, $k_B$ the Boltzmann constant, $\mathcal{P}(T)$ the radiative losses per unit emission measure, $\mathcal{Q}(s,t)$ the input heating power per unit volume.

We solve these equations numerically by means of the Palermo-Harvard hydrodynamic code (Peres et al. 1982, Betta et al. 1997), now able to obtain solutions with high resolution all over the corona and even in the thin and moving transition region, thanks to an adaptive regridding. Given the symmetry of the present problem, the code used solves the equations on one half of the loop, but a more recent version of the code can now solve also asymmetric problems.

The heating source is modeled as the sum of a steady heating term - which would maintain the initial corona in steady conditions outside the flare - and a transient heating which triggers the flare.

The initial atmosphere is in hydrostatic equilibrium and consists of a transition region and a corona calculated according to Serio et al. (1981) for $T > 2 \times 10^4$ K, and of a chromosphere according to Vernazza et al. (1980), carefully matched together at $T = 2 \times 10^4$ K.

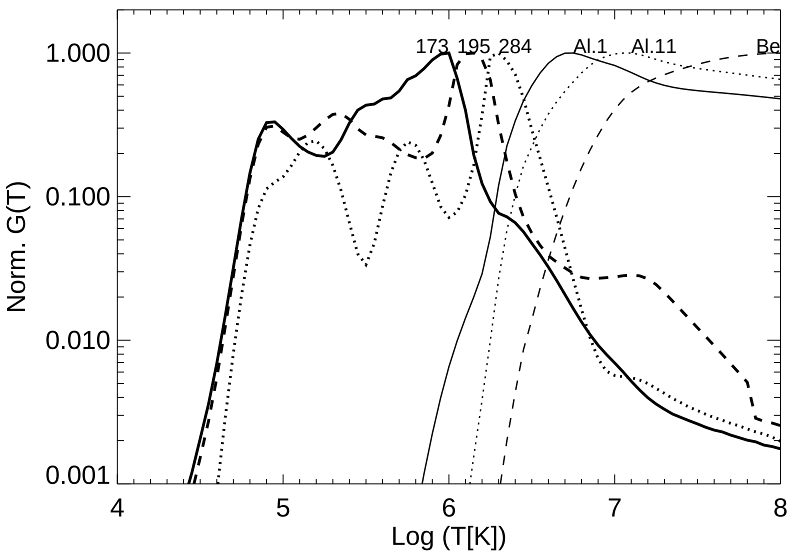


Figure 1. Coronal plasma emissivity per unit emission measure G(T) vs. temperature folded through the TRACE (*thick lines*) and Yohkoh SXT (*thin lines*) spectral response. Different curves pertain to the labelled different filters.

The code provides the evolution of the density, temperature and velocity along the model loop. These quantities are then used to obtain the brightness of the loop as would be detected by a given instrument:

$$\mathcal{B}(s,t) = n^2(s,t)G(T(s,t)) \tag{5}$$

where $G(T)$ is the plasma emissivity folded through the instrumental response per unit emission measure. For this synthesis we use the Analysis System of Astrophysical Plasmas (ASAP, Maggio et al. 1994).

In Fig.1 we show the functions $G(T)$ for TRACE (bands with a maximum around 173 Å, 195 Å and 284 Å) and Yohkoh SXT (thin and thick Al, Be filters). TRACE is clearly sensitive to the emission of cooler plasma ($\sim 10^6$ K) than Yohkoh SXT ($\geq 3\ 10^6$ K).

## 3. The model flare

Let's now consider a specific model flare and explore how it would look like if observed with Yohkoh SXT and TRACE. The flare occurs in a typical active region loop with half-length $L = 2 \times 10^9$ cm and base pressure $p_0 = 6$ dyne cm$^{-2}$, yielding a maximum temperature (at the apex) $T_0 = 3.2 \times 10^6$ K. It is triggered by a Gaussian-shaped heating deposition:

$$\mathcal{Q}(s,t) = H_0\ f(t)\ g(s) \quad . \tag{6}$$

$$g(s) = \exp\left[-\frac{(s-s_0)^2}{2\sigma^2}\right] \tag{7}$$

where $s_0$ is the position of the heating maximum intensity, with $H_0 = 10$ erg cm$^{-3}$ s$^{-1}$ and $\sigma = 5 \times 10^8$ cm, centered at the loop apex, kept constant ($f(t) = 1$) for 3 minutes. These parameters have been used in the past to model specific flares and yield a flare peaking at $T_{max} \approx 20$ MK.

The plasma evolution for this model flare is well-known from previous work (Peres et al. 1987, Peres & Reale 1993, Reale & Peres 1995). Let's consider the first three minutes only (the flare rising phase). As shown in Fig.2, the temperature rapidly increases all along the loop, because a very fast conduction front propagates from the apex to the footpoints, and saturates to a steady value between 10 MK in the lower part of the flaring corona and 20 MK at the apex of the loop. The density instead remains steady in the first 10 seconds, and then, due the expansion of the lower-lying chromosphere overheated by the strong conduction front, increases first with a front propagating from the footpoints (chromospheric evaporation) and more gently and uniformly after 1 minute.

The combined evolution of temperature and density determines the evolution of the plasma emission, but the final appearance as would be observed depends also on the folding through the instrument response. In fact let's first consider the evolution of the emission distribution along the loop as would be detected by Yohkoh SXT, shown in Fig.3, left panel. The brightness is initially uniformly low in the Be filter band. A first sudden enhancement of two orders of magnitude is due to the temperature increase. Then the further brightness front of the chromospheric evaporation propagates from the footpoints. After 180 sec the brightness is again uniform but four orders of magnitude higher than that of the initial active region loop.

As anticipated, we find significant differences with respect to the evolution as detected by TRACE in the 195 Å band (Fig. 3, right panel). First of all the brightness is never uniform along the loop, the footpoints being brighter than the apex practically at any time. Curiously the initial temperature enhancement produces a decrease in the loop brightness, because the temperature goes far from the peak of instrument sensitivity. The subsequent brightness enhancement is therefore uniquely due to the increase of the emission measure. After 180 sec the brightness is only about 20 times higher than at the beginning.

We sketch how the loops would look like, by integrating the brightness on the respective pixel sizes (2.45" for SXT, 0.5" for TRACE). In Fig.4, the loop brightness in the SXT Be filter band is shown every 5 sec since the beginning of the simulation. The logarithmic grey scale is the same for all pictures and includes three decades. After an initial dishomogeneity (between 15 and 45 sec) due to the chromospheric evaporation, the loop becomes quite uniformly bright. Incidentally, this is not entirely consistent with many flare observations which typically show a long-lasting brightening at the loop apex. This feature at present has not been explained with loop hydrodynamic modeling (Reale & Peres 1995, Hori et al. 1997). The initial loop is invisible in the chosen grey scale.

The model flaring loop appears very different when looked in the TRACE 195 Å band (Fig.5). In the chosen grey scale including three decades, the loop is never entirely visible in the three minutes studied, although larger and larger

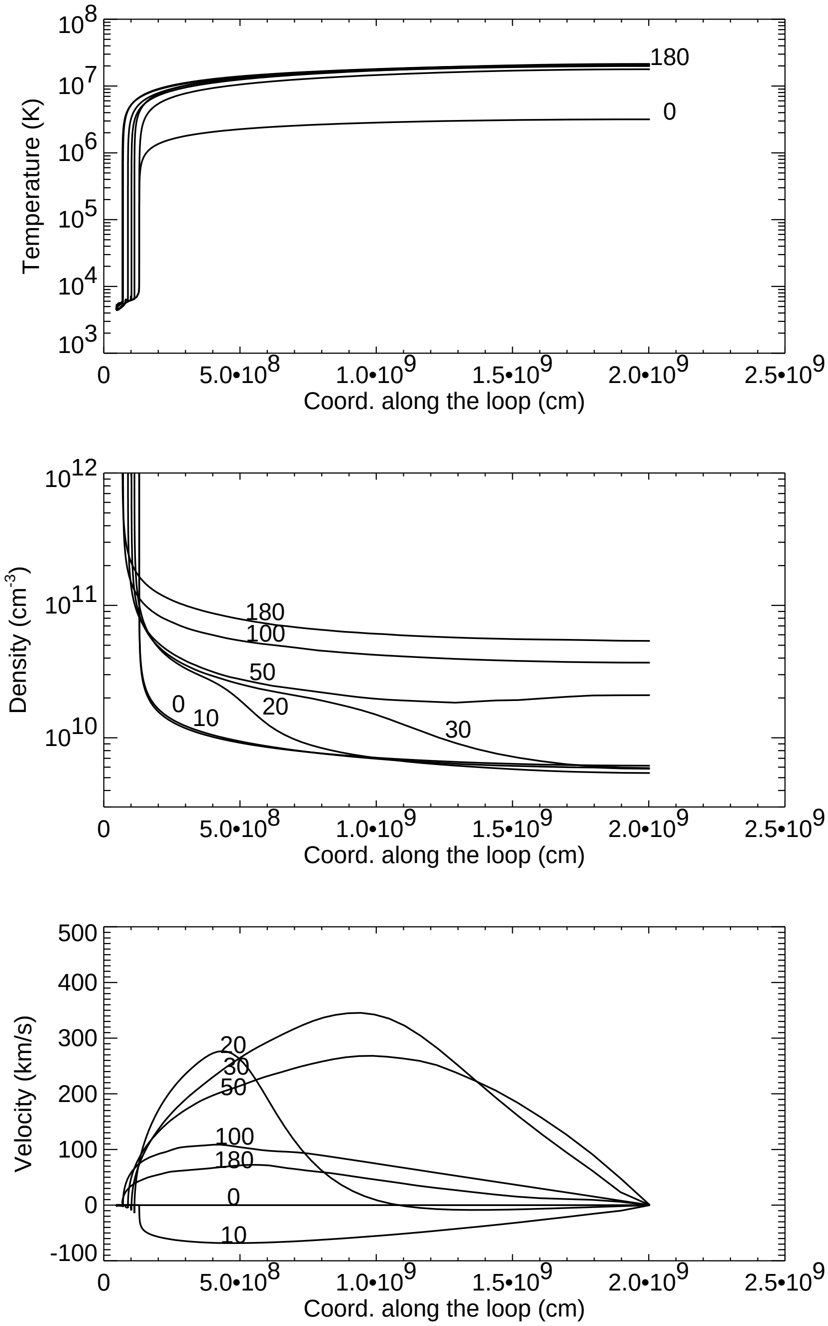


Figure 2. Evolution of temperature, density and velocity along the loop predicted by the hydrodynamic modeling of a flare in the active region loop described in the text. Distributions sampled at the labelled times (seconds since the beginning of the flare) along half loop are shown, the origin begin at the loop footpoint.

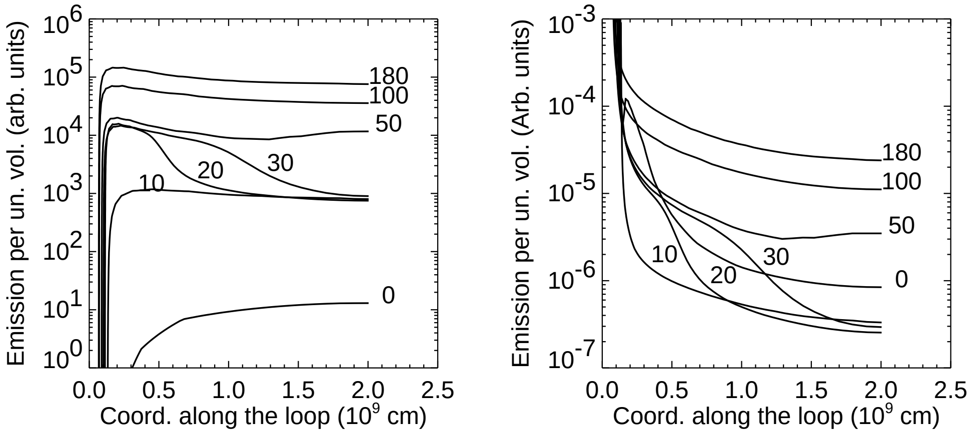


Figure 3. Evolution of the emission per unit volume along the model flaring loop of Fig. 2 detected by Yohkoh SXT in the Be filter (*left panel*) and by TRACE in the 195 Å band (*right panel*), at sampled times (seconds).

portions become visible with time. The footpoints are always very bright. Interestingly, at variance with Yohkoh SXT, the base of the loop is visible since the very beginning. This means that flare observations with TRACE should not require a large dynamic range, i.e. a switch to a flaring mode and progressively shorter exposures.

## 4. Discussion and conclusions

The above results show how the physical interpretation of X-ray observations can be untrivial and how hydrodynamic loop modeling in this respect can provide a very useful tool. In particular it has been shown that coronal loops, and specifically flaring loops, can look very different both in structure and evolution if observed by instruments with different spectral bands. As an example we have analyzed a model flare in a typical active region loop as would be observed with two presently interesting telescopes, Yohkoh SXT and TRACE. As a result the Be filter of Yohkoh SXT in flaring mode appears to be very appropriate to observe the global properties and evolution of the flaring loop, due to its wide and high-temperature response. On the other hand TRACE appears to be able to monitor a flaring loop with no need to switch to a specific flaring mode, which may be a very important issue for observing the fast and difficult to capture flare rising phase.

Such hints could be obtained only thanks to hydrodynamic modeling coupled to emission synthesis, which can provide a detailed diagnostic of plasma physical conditions, evolution and dynamics and quantitative suggestions for the interpretation.

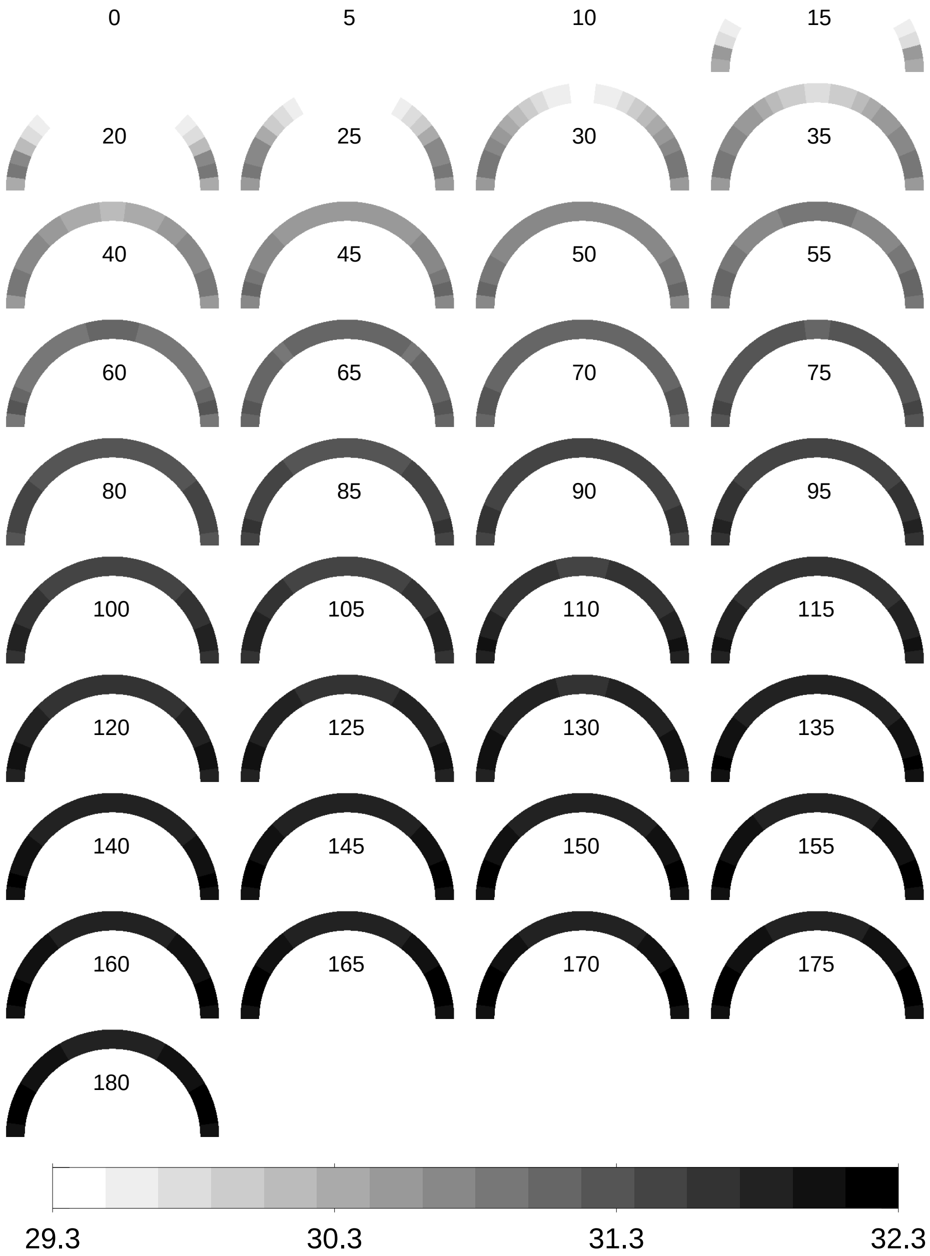


Figure 4. Loop brightness during the model flare expected in the Yohkoh SXT Be filter band (log (SXT Digital Numbers $10^{-46}$ cm$^{-2}$ s$^{-1}$). Time is in seconds since the beginning of the hydrodynamic simulation. The grey scale is the same for all loop pictures and includes three decades.

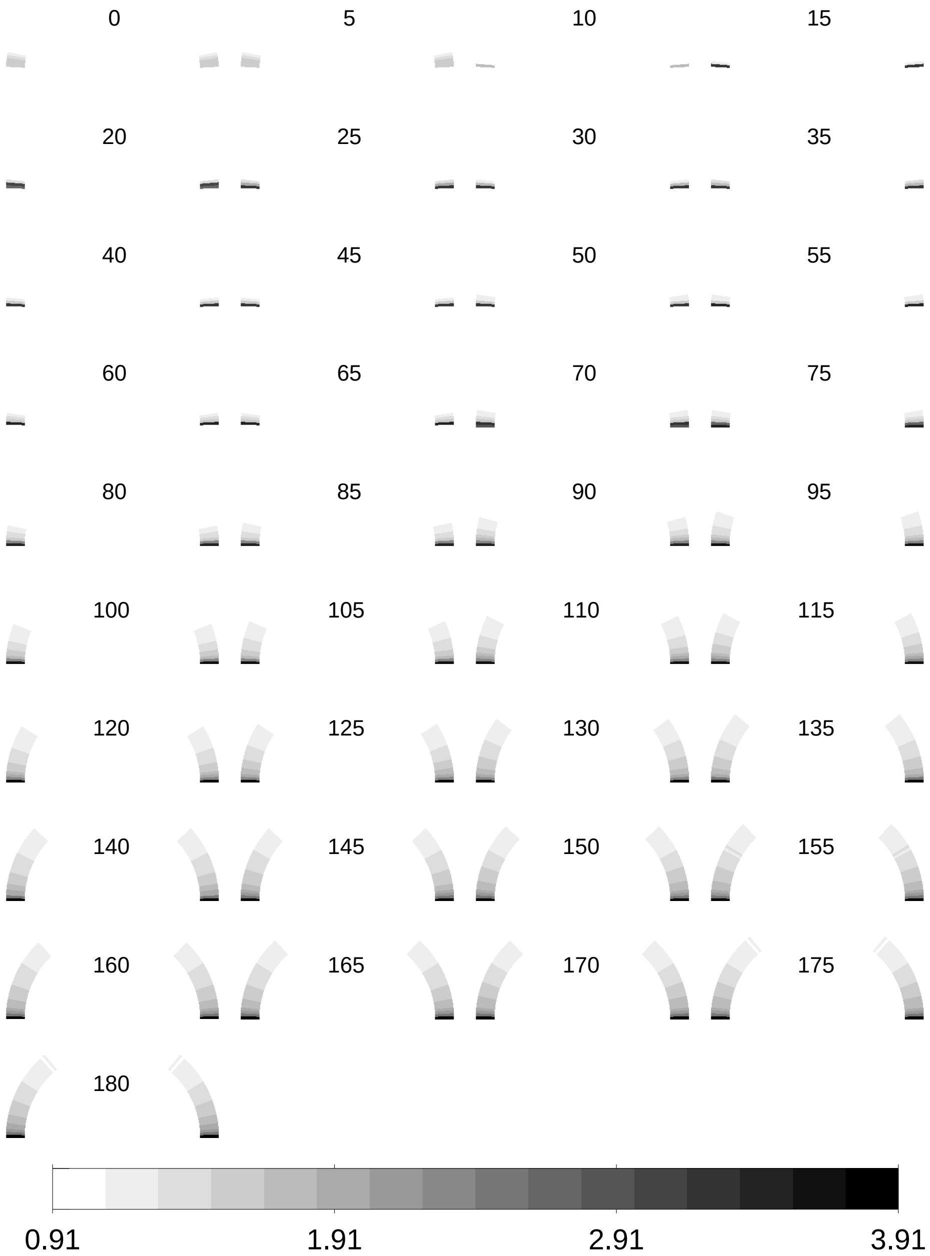


Figure 5. Same as Fig.4 but in the TRACE 195 Å band (log erg cm$^{-2}$ s$^{-1}$).

**Acknowledgments.** We acknowledge partial support from Ministero della Università e della Ricerca Scientifica e Tecnologica, Agenzia Spaziale Italiana and Consiglio Nazionale delle Ricerche.

## References

Betta R. M., Peres G., Serio S., Reale F., 1997, A&ASuppl., 122, 585.

Hori K., Yokoyama T., Kosugi T., Shibata K., 1997, ApJ, submitted.

Kopp R.A., Fisher G.H., MacNeice P., McWhirter R.W.P., Peres G., 1986, NASA CP-2439, Energetic Phenomena on the Sun, Kundu and Woodgate, eds.

Maggio A., Reale F., Peres G., Ciaravella A., 1994, Comp. Phys. Comm. 81, 105.

Peres G., Reale F., 1993, A&A, 267, 566.

Peres G., Reale F., Serio S., Pallavicini R., 1987, ApJ, 312, 895.

Peres G., Rosner R., Serio S., Vaiana G. S., 1982, ApJ, 252, 791.

Raymond J. C., Smith B. W., 1977, ApJS, 35, 419.

Reale F., Peres G., 1995, A&A, 299, 225.

Serio S., Peres G., Vaiana G. S., Golub L., Rosner R., 1981, ApJ, 243, 288.

Vernazza J. E., Avrett E. H., Loeser R., 1980, ApJS, 45, 619.